

Synthesis, Antibacterial Properties and Molecular Docking of Nitrobenzoylthiourea Compounds and their Copper(II) Complex

NURINA ASYURA BINTI MOHD YUNUS¹, MAYA ASYIKIN MOHAMAD ARIF^{1*} & FAZIA MOHAMAD SINANG^{2*}

¹Chemistry Programme, Faculty of Resource Science and Technology, Universiti Malaysia Sarawak, 94300 Kota Samarahan, Sarawak, Malaysia; ²Resource Biotechnology Programme, Faculty of Resource Science and Technology, Universiti Malaysia Sarawak, 94300 Kota Samarahan, Sarawak, Malaysia

*Corresponding authors: mamasyikin@unimas.my; msfazia@unimas.my

Received: 21 February 2024 Accepted: 25 September 2024 Published: 31 December 2024

ABSTRACT

The rise of multidrug-resistant microbial pathogens has increased the demand for highly effective antibiotics. Five nitrobenzoylthiourea ligands (**1–5**) with amino acid side chains and their corresponding Cu(II) complexes (**6–10**) were synthesised with yields ranging from 43% to 90%. The successful synthesis of ligands **1–5** were confirmed by the absence of the $\nu(\text{NCS})$ stretching band and the presence of the $\nu(\text{NH})$ band, indicating the complete reaction of all (NCS) with a series of amino acids as well as the appearance of two N-H signals in the ¹H NMR spectra of all the synthesised ligands. On the other hand, the shift of the (C=O) carboxylic peaks in the Cu(II) complexes suggested successful coordination of ligands to the metal ion *via* the carboxylate group. The antibacterial activities of these compounds were tested against six bacteria: *Staphylococcus aureus*, *Bacillus cereus*, *Listeria monocytogenes*, *Escherichia coli*, *Klebsiella pneumoniae*, and *Pseudomonas aeruginosa* using the disc diffusion method. The Cu(II) complexes (**6–10**) exhibited enhanced antibacterial activity compared to the ligands (**1–5**), especially against gram-negative bacteria (*E. coli*, *K. pneumoniae*, and *P. aeruginosa*). For example, compound **4** showed moderate activity against *K. pneumoniae* with a 14 mm inhibition zone while its Cu(II) complexes, **8** recorded better inhibition against *K. pneumoniae* with a 16 mm inhibition zone. Molecular docking studies on all complexes (**6–10**) also revealed higher binding affinity with targeted proteins with binding energy between -10.4 kcal/mol to -9.0 kcal/mol, in comparison with ligand **2** and **4** with the binding energy of only -7.7 kcal/mol (against *S. aureus*) and -6.9 kcal/mol (against *K. pneumoniae*). The enhanced antibacterial activity of all complexes correlates with the higher binding affinity obtained for all complexes. Hence, this study concludes that the nitrobenzoylthiourea derivatives, and particularly their Cu(II) complexes can show potential as antibacterial agent although more thorough investigation are required to develop these compounds into useful drugs.

Keywords: Antibacterial agents, binding affinity, Cu(II) complexes, nitrobenzoylthiourea

Copyright: This is an open access article distributed under the terms of the CC-BY-NC-SA (Creative Commons Attribution-NonCommercial-ShareAlike 4.0 International License) which permits unrestricted use, distribution, and reproduction in any medium, for non-commercial purposes, provided the original work of the author(s) is properly cited.

INTRODUCTION

The discovery of new medications has accelerated in recent decades as the prevalence of germs resistant to antibiotics has increased (Fair & Tor, 2014). This is due the negligent use of antibiotic, which resulted in the evolution of multidrug resistance bacteria (Mohler *et al.*, 2017). Microorganisms develop a variety of mechanisms to limit antimicrobial efficiency, including altering target sites, decreasing cellular permeability to allow for drug penetration, enzymatic destruction of antimicrobial substances, and biofilm development (Idrees *et al.*, 2020). As a result, demand for highly resistant antibiotics increased, and it is critical to conduct rapid

evaluations of potential drugs. On the other hand, the vast array of biological activities of the thiourea-based compound has sparked considerable interest among researchers, with the expectation that modification of ligands and their coordination *via* metal ions would increase their resistance to multidrug-resistant microbial pathogens and influence the drug's microbiological properties. Moreover, metal ions are positively charged and act as electrophiles whereas biological molecules such as DNA and protein are electron-rich and tend to bind and interact with biological molecules (Boros *et al.*, 2020).

Thiourea derivatives have garnered considerable attention as versatile ligands in a variety of applications due to their unique ability

to coordinate with a variety of transition metal ions as monodentate or bidentate ligands and to coordinate with metal centres as neutral, monoanionic, or dianionic ligands to form a stable complex (Wakshlak *et al.*, 2015; Mohapatra *et al.*, 2021). The ability of multiband coordination is dependent on the presence of a donor heteroatom such as oxygen, nitrogen or sulphur, in the ligand. With the presence of two units of reactive primary amide group, thiourea has been found to be a suitable precursor in the synthesis of a variety of their derivatives as well as an excellent chelating agent to metals through S and O, and it has demonstrated a wide range of biological activity, including antibacterial and antifungal activity (Ikoko *et al.*, 2015; Mohapatra *et al.*, 2021). Thiourea functionality as versatile precursor derives from its ability to form stable hydrogen bonds with recognition elements of biological targets, including proteins, enzymes and receptor as the hydrogen bond network is essential for stabilizing ligand-receptor interaction (Ronchetti *et al.*, 2021). Consequently, reactive functional groups of thiourea, such as amino, imino, and thiol, can play important roles as precursor in the synthesis of organic molecules for various biological applications, as demonstrated in bacteriostatic activities, where they can be protonated under acidic conditions and reacted with the carboxyl and phosphate groups of the bacterial surface, resulting in prominent antibacterial activity (Ngaini *et al.*, 2012; Halim & Ngaini, 2017). Additionally, thiourea is employed as an active ingredient in pharmaceuticals, which increases the usability of their derivatives as they will pose no adverse risk to natural living bodies (Ohammad, 2018).

Metal complexes are thought to exert their effect through the inhibition of enzymes, interaction with intracellular biomolecules, increased lipophilicity and modification of cell membrane functions (Malik *et al.*, 2018). Metal complex considerably improved the results given by thiourea ligand alone. On the other hand, copper(II) was specifically chosen due to its well-known antimicrobial properties. Copper exposure has been shown to impair the integrity of the bacterial cell wall, resulting in the microorganism's mortality (Montero *et al.*, 2019), while also increasing their susceptibility to copper ions, which cause metabolic dysfunction. According to Arendsen and coworkers (2019), when copper ions reach a

critical intracellular concentration, the plasma membrane becomes increasingly permeable, allowing important cell content including nucleotides, amino acids, and potassium. Moreover, attachment of amino acids may be advantageous as these are biomolecules that play a critical role in a variety of biological functions (Raheel *et al.*, 2016) and have been used to enhance the efficacy (*in vitro*) of existing drugs (Idrees *et al.*, 2020).

In this study, five new monobenzoyl thiourea derivatives were synthesised *via* the reaction of 4-nitrobenzoyl isothiocyanate with tryptophan, methionine, valine, alanine, and cysteine. The effect of complexation with copper(II) metal in their antibacterial activity was analysed against three gram-positive and three gram-negative bacteria. The contribution of newly synthesised nitrobenzoyl thiourea bearing amino acid side chain and their copper(II) complexes in the antibacterial study were emphasised with molecular docking analysis. Even if the incorporation of copper(II) ion does not improve the antibacterial activity directly, it may lead to compounds that can potentially inhibit virulence mechanisms of highly resistant pathogens as this study is important in drug discovery for the medical industry.

MATERIALS & METHODS

Materials

4-nitrobenzoyl chloride, potassium thiocyanate (KSCN) powder, tryptophan, methionine, serine, valine, L-alanine, cysteine, silver(I) nitrate, copper(II) chloride, potassium hydroxide (KOH), distilled acetone, ethanol, acetonitrile, ethyl acetate, propanol, methanol, hexane, dichloromethane, chloroform, cyclohexanol, nitromethane, tetrahydrofuran, diethyl ether, toluene, petroleum ether is of reagent grade and used without purification. Acetone was distilled over magnesium sulfate anhydrous.

Instrumentation and Analytical Characterisation of Thiourea Compounds

Characterisation of pure thiourea compounds were conducted using Fourier Transform Infrared Spectrometry (FTIR) Perkin-Elmer Spectrum (GX2000) spectrometer. The FTIR spectra (ν/cm^{-1}) of all compounds were determined using Attenuated Total Reflection

(ATR) technique. The CHNS elemental analysis of thiourea ligands and complexes were performed using Thermo Scientific™ FlashSmart™ Elemental Analyser. The ^1H and ^{13}C NMR spectroscopy (JEOL ECA 500 MHz) were used to confirm the chemical structure of thiourea ligands by identifying the H and C present in the synthesised compounds. All NMR spectra were recorded in DMSO- d_6 solutions and the chemical shifts were reported in δ (ppm).

Synthesis of Thiourea Ligands

Synthesis of ((4-nitrobenzoyl)carbamothioyl)tryptophanato (1)

4-nitrobenzoyl chloride (0.01 mol, 1.86 g) and potassium thiocyanate (0.01 mol, 0.97 g) were dissolved in 120 mL of distilled acetone. The solution was stirred for 1 hour until white precipitate formed. The white precipitate, potassium chloride (KCl) was removed while the filtrate formed was kept for the next step. A 0.01 mol (2.04 g) of tryptophan was added to the filtrate solution and the solution mixture was heated to reflux for three days (72 hours) at 65 °C before being filtered, ultimately yielding only the targeted compounds while eliminating unwanted products. The mixture was allowed to cool at room temperature and the filtrate was left to evaporate at room temperature for several days. After several days, orange solid was formed and collected as compound **1** (3.357 g, 81.40%). Compound was purified by recrystallisation using ethanol/dichloromethane (2:1) ratio. FTIR ν_{max} 3412 (N-H), 1717 (C=O carboxylic), 1674 (C=O amide), 1514 (C=C aromatic), 854 (C=S), 1159 (C-N). Calcd. for ($\text{C}_{19}\text{H}_{16}\text{N}_4\text{O}_5\text{S}$); C: 55.33%, H: 3.91%, N: 13.58%, S: 7.77%, found: C: 55.72%, H: 4.18%, N: 13.87%, S: 6.51%. ^1H NMR (500 MHz; DMSO- d_6) δ 11.89 (1H, s, NH), 11.04 (1H, d, J = 7.6 Hz, NH), 10.92 (1H, d, NH), 8.28 (2H, d, J = 4.6 Hz, Ar-H), 8.03 (2H, d, J = 1.5 Hz, Ar-H), 7.49 (1H, d, J = 7.6 Hz, Ar-H), 7.29 (1H, d, J = 7.6 Hz, Ar-H), 7.14 (1H, d, J = 2.3 Hz, Ar-H), 7.01 (1H, t, J = 7.6 Hz, Ar-H), 6.90 (1H, t, J = 7.6 Hz, Ar-H), 2.47 (1H, q, J = 1.8 Hz, CH), 2.06 (2H, d, J = 6.1 Hz, CH_2). ^{13}C -NMR (125 MHz; DMSO- d_6) δ 180.2 (C=SNH), 172.3 (C=OOH), 167.5 (C=ONH), 150.3 (Ar-C), 138.5 (Ar-C), 136.6 (Ar-C), 130.7 (Ar-C), 127.9-108.9 (Ar-C), 58.9 (CH), 26.7 (CH_2).

Synthesis ((4-nitrobenzoyl)carbamothioyl)

methioninato (2)

The procedure for compound **1** was repeated using methionine (0.01 mmol, 1.49 g). After several days, yellow solid was formed and collected as compound **2** (2.899 g, 81.11%). Compound was purified through washing with distilled water. FTIR ν_{max} 3218 (N-H), 1722 (C=O carboxylic), 1508 (C=O amide), 1508 (C=C aromatic), 853 (C=S), 1156 (C-N). Calcd. for ($\text{C}_{13}\text{H}_{15}\text{N}_3\text{O}_5\text{S}_2$); C: 43.69%, H: 4.23%, N: 11.76%, S: 17.94%, found: C: 43.71%, H: 4.22%, N: 11.82%, S: 17.76%. ^1H NMR (500 MHz; DMSO- d_6) δ 11.88 (1H, s, NH), 11.09 (1H, d, J = 7.4 Hz, NH), 8.27-8.31 (2H, m, Ar-H), 8.09-8.12 (2H, m, Ar-H), 4.97 (1H, dd, J = 12.6, 6.9 Hz, CH), 2.51 (2H, q, J = 7.5 Hz, CH_2), 2.46 (2H, t, J = 1.7 Hz, CH_2), 2.03 (3H, s, CH). ^{13}C -NMR (125 MHz; DMSO- d_6) δ 180.7 (C=SNH), 172.3 (C=OOH), 167.4 (C=ONH), 150.3 (Ar-C), 138.2 (Ar-C), 130.8 (Ar-C), 123.8 (Ar-C), 57.2 (CH), 30.9 (CH_2), 29.7 (CH_2), 15.2 (CH_3).

Synthesis of ((4-nitrobenzoyl)carbamothioyl)valinato (3)

The procedure for compound **1** was repeated using valine (0.01 mol, 1.17 g). After several days, milky white solid was formed and collected as compound **3** (2.912 g, 89.51%). Compound was purified by recrystallisation using propanol/dichloromethane (2:1) ratio. FTIR ν_{max} 3237 (N-H), 1716 (C=O carboxylic), 1672 (C=O amide), 1521 (C=C aromatic), 854 (C=S), 1163 (C-N). Calcd. for ($\text{C}_{13}\text{H}_{15}\text{N}_3\text{O}_5\text{S}$); C: 47.99%, H: 4.65%, N: 12.92%, S: 9.86%, found: C: 48.06%, H: 4.73%, N: 12.97%, S: 8.26%. ^1H NMR (500 MHz; DMSO- d_6) δ 11.93 (1H, s, NH), 11.17 (1H, d, J = 7.7 Hz, NH), 8.28 (2H, d, J = 8.9 Hz, Ar-H), 8.11 (2H, d, J = 8.9 Hz, Ar-H), 2.46 (1H, t, J = 1.7 Hz, CH), 2.27-2. (1H, m, CH), 0.91-0.98 (6H, m, 2 CH_3). ^{13}C -NMR (125 MHz; DMSO- d_6) δ 181.1 (C=SNH), 171.8 (C=OOH), 167.8 (C=ONH), 150.4 (Ar-C), 138.4 (Ar-C), 130.8 (Ar-C), 123.8 (Ar-C), 63.2, 30.7 (CH), 19.2, 18.6 (CH_3).

Synthesis of ((4-nitrobenzoyl)carbamothioyl)alaninato (4)

The procedure for compound **1** was repeated using alanine (0.01 mol, 0.89 g). After several days, orange-brick solid was formed and

collected as compound **4** (2.363 g, 79.5%). Compound was purified by recrystallisation using ethanol/dichloromethane (2:1) ratio. FTIR ν_{\max} 3281 (N-H), 1709 (C=O carboxylic), 1659 (C=O amide), 1532 (C=C aromatic), 847 (C=S), 1167 (C-N). Calcd. for (C₁₁H₁₁N₃O₅S); C: 44.44%, H: 3.73%, N: 14.13%, S: 10.79%, found: C: 44.84%, H: 3.97%, N: 14.58, S: 8.68%. ¹H-NMR (500 MHz, DMSO-d₆) δ 11.88 (1H, s, NH), 11.11 (1H, d, *J* = 6.9 Hz, NH), 8.28 (1H, d, *J* = 8.9 Hz, Ar-H), 8.09 (1H, d, *J* = 8.9 Hz, Ar-H), 4.83-4.77 (1H, m, CH), 1.46 (3H, d, *J* = 7.2 Hz, CH₃). ¹³C-NMR (125 MHz, DMSO-d₆) δ 180.1 (C=SNH), 173.4 (C=OOH), 167.6 (C=ONH), 150.3 (Ar-C), 138.5 (Ar-C), 130.7 (Ar-C), 123.9 (Ar-C), 17.7 (CH₃).

Synthesis of ((4-nitrobenzoyl)carbamothioyl) cysteinato (5)

The procedure for compound **1** was repeated using cysteine (0.01 mol, 1.2116 g). After several days, orange solid was formed and collected as compound **5** (2.706 g, 82.15%). Compound was purified by recrystallisation using ethanol/hexane (1:2). FTIR ν_{\max} 3113 (N-H), 1716 (C=O carboxylic), 1668 (C=O amide), 1519 (C=C aromatic), 848 (C=S), 1157 (C-N). Calcd. for (C₁₁H₁₁N₃O₅S₂); C: 40.11%, H: 3.37%, N: 12.76%, S: 19.47%, found: C: 40.43%, H: 3.57%, N: 14.07%, S: 16.49%. ¹H-NMR (500 MHz, DMSO-d₆) δ 11.90 (1H, s, NH), 11.21 (1H, d, *J* = 7.4 Hz, NH), 8.27 (1H, d, *J* = 5.2 Hz, Ar-H), 8.09 (1H, d, *J* = 8.9 Hz, Ar-H), 3.57 (1H, dd, *J* = 11.7, 9.5 Hz, CH), 2.46 (2H, t, *J* = 1.9 Hz, CH₂). ¹³C-NMR (125 MHz; DMSO-d₆) δ 172.4 (C=SNH), 166.3 (C=OOH), 149.9 (C=ONH), 142.3 (Ar-C), 136.9 (Ar-C), 130.6 (Ar-C), 124.0 (Ar-C), 57.2 (CH), 32.9 (CH₂).

Synthesis of Copper(II) Complexes of Thiourea

Synthesis and Characterisation Data of di((4-nitrobenzoyl)carbamothioyl) tryptophanato copper(II) (6)

Compound **1** (0.206 g, 0.5 mmol) was dissolved in 10 ml of ethanol followed by continuous stirring to make sure all ligand was dissolved. A (2.2 mL 0.5 mmol) of KOH was added into the solution and the mixture was stirred at room temperature for 30 minutes. A metal solution of CuCl₂.2H₂O (0.043 g, 0.25 mmol) in 2 mL of

distilled water was later added into the solution containing ligand and KOH before the mixture was stirred for another 24 hours. Then, the mixture was filtered out and left to evaporate for few days to give out brownish precipitate of complex **6** (0.18 g, 68.70%). The complex was then subjected to purification with distilled water. FTIR ν_{\max} 3170 (N-H), 1681 (C=O amide), 1520 (C=C aromatic), 853 (C=S), 1171 (C-N). Calcd. for (C₃₈H₄₈CuN₈O₁₉S₂); C: 43.53%, H: 4.61%, N: 10.69%, S: 6.12%, found: C: 43.16%, H: 3.85%, N: 10.62%, S: 6.61%.

Synthesis and Characterisation Data of di((4-nitrobenzoyl)carbamothioyl)methionato copper(II) (7)

The procedure for the synthesis of complex **7** was repeated using ligand **2** (0.357 g, 1.0 mmol), KOH (4.7 mL 1.0 mmol) and CuCl₂.2H₂O (0.085 g, 0.5 mmol). After few days, green precipitate of complex **7** (0.239 g, 57.59 %) was obtained. FTIR ν_{\max} 2986 (N-H), 1682 (C=O amide), 1523 (C=C aromatic), 854 (C=S), 1169 (C-N). Calcd. for (C₂₆H₃₄CuN₆O₁₃S₄); C: 37.61%, H: 4.13%, N: 10.12%, S: 15.45%, found: C: 37.25%, H: 3.73%, N: 10.52%, S: 15.61%.

Synthesis of di((4-nitrobenzoyl)carbamothioyl)valinatocopper(II) (8)

The procedure for the synthesis of complex **8** was repeated using compound **3** (0.325 g, 1.0 mmol), KOH (4.7 mL 1.0 mmol) and CuCl₂.2H₂O (0.085 g, 0.5 mmol). After few days, brownish precipitate of complex **8** (0.261 g, 65.10%) was obtained. FTIR ν_{\max} 2964 (N-H), 1679 (C=O amide), 1519 (C=C aromatic), 853 (C=S), 1166 (C-N). Calcd. for (C₂₆H₃₈CuN₆O₁₅S₂); C: 38.92%, H: 4.77%, N: 10.48%, S: 7.99%, found: C: 48.73%, H: 4.30%, N: 10.85%, S: 9.21%.

Synthesis of di((4-nitrobenzoyl)carbamothioyl)alaninatocopper(II) (9)

The procedure for the synthesis of complex **9** was repeated using compound **4** (0.193 g, 0.65 mmol), KOH (3.1 mL 0.65 mmol) and CuCl₂.2H₂O (0.0554 g, 0.325 mmol). After few days, brownish precipitate of complex **9** (0.137 g, 55.24%) was obtained. FTIR ν_{\max} 3116 (N-H), 1671 (C=O amide), 1519 (C=C aromatic), 854 (C=S), 1170 (C-N). Calcd. for

(C₂₂H₃₂CuN₆O₁₆S₂); C: 34.58%, H: 4.22%, N: 11.00%, S: 8.39%, found: C: 34.30%, H: 3.90%, N: 11.04%, S: 9.89%.

Synthesis of di((4-nitrobenzoyl)carbamothioyl)tcysteinatocopper(II) (10)

The procedure for the synthesis of complex **10** was repeated using compound **5** (0.157 g, 0.48 mmol), KOH (2.3 mL, 0.48 mmol) and CuCl₂·2H₂O (0.041 g, 0.24 mmol). After few days, brownish precipitate of complex **10** (0.131 g, 76.15%) was obtained. FTIR ν_{\max} 3072 (N-H), 1703 (C=O carboxylic), 1651 (C=O amide), 1523 (C=C aromatic), 851 (C=S), 1168 (C-N). Calcd. for (C₂₂H₂₀CuN₆O₁₀S₄); C: 36.69%, H: 2.80%, N: 11.67%, S: 17.81%, found: C: 36.64%, H: 3.08%, N: 12.26%, S: 12.75%.

Antimicrobial Activity Test

All synthesised compounds were evaluated for antibacterial activity using the disc diffusion method against three gram-positive bacteria (*Staphylococcus aureus*, *Bacillus cereus*, *Listeria monocytogenes*) and three gram-negative bacteria (*Escherichia coli*, *Klebsiella pneumoniae*, *Pseudomonas aeruginosa*). All bacteria were cultured in Mueller Hinton broth and incubated at 37 °C with stirring for 24 hours. The bacterial suspension was adjusted to 0.5 McFarland standard and 20 μ L of the inoculum was spread uniformly onto Mueller Hinton agar using a sterile cotton swab. The disc with different concentrations (50 ppm, 100 ppm, 150 ppm, 200 ppm, 250 ppm, 500 ppm and 1000 ppm) of synthesized compounds dissolved in DMSO were placed onto the Mueller Hinton agar. The DMSO was used as negative control (Halim & Ngaini, 2016). Meanwhile, penicillin, vancomycin, ampicillin, tetracycline, ceftazidime and imipenem were used as the standard antibiotic for *Staphylococcus aureus*, *Bacillus cereus*, *Listeria monocytogenes*, *Escherichia coli*, *Klebsiella pneumoniae*, *Pseudomonas aeruginosa* respectively. Each antibiotic was selected based on its established efficacy as a standard treatment for the corresponding bacterial strain. Subsequently, the plates were incubated at 37 °C for 24 hours. After the incubation, the clear inhibition zone was observed, and the diameter of the inhibition zone was measured in millimetre (mm).

Molecular Docking Study

The crystal structures of the targeted bacterial proteins, *S. aureus* (PDB entry: 4xwa), *B. cereus* (PDB entry: 5bca), *K. pneumoniae* (PDB entry: 5xun), and *P. aeruginosa* (PDB entry: 7ci4) were retrieved in PDB format from the RCSB Protein Data Bank. The protein was prepared using AutoDock Tools-1.5.7 by adding polar hydrogen atoms, removing water molecules, and ensuring the structure was appropriately formatted. The prepared protein structure was saved as a pdbqt file. The synthesised ligand structures were generated using Chemdraw software and were later converted to pdbqt files using a variety of software programs, including Molview, Open Babel, and the AutoDock Tools program. Docking simulations were performed with AutoDock Vina using default grid box parameters (40 \times 40 \times 40, 0.375 Å spacing) provided by AutoDock Tools (Trott & Olson, 2010). These parameters automatically center the grid on the protein's binding pocket. The grid coordinates were (14.743, -0.047, 14.858) for *S. aureus*, (40.132, 23.825, 36.938) for *B. cereus*, (-28.095, 7.000, 19.029) for *K. pneumoniae*, and (26.335, -8.649, 21.505) for *P. aeruginosa*. These default settings are designed to maximise the likelihood of identifying potential binding interactions across the protein surface, particularly in exploratory docking studies where the exact binding site may not be well-defined. Following that, molecular docking was performed using AutoDock Vina (Pingaew *et al.*, 2018), which efficiently handles the docking process within the grid parameters. The docking process was managed with command prompt, and the binding poses were visualized with PyMOL (Schrodinger, 2016), an open-source molecular visualization tool used to identify hydrogen bonds and other key interactions between the synthesised compounds and amino acid residues of the protein (Roche Allred *et al.*, 2017). Factors such as the conformation within protein binding site, binding affinity, and the number of hydrogen bond interactions with protein residues were investigated for better understanding.

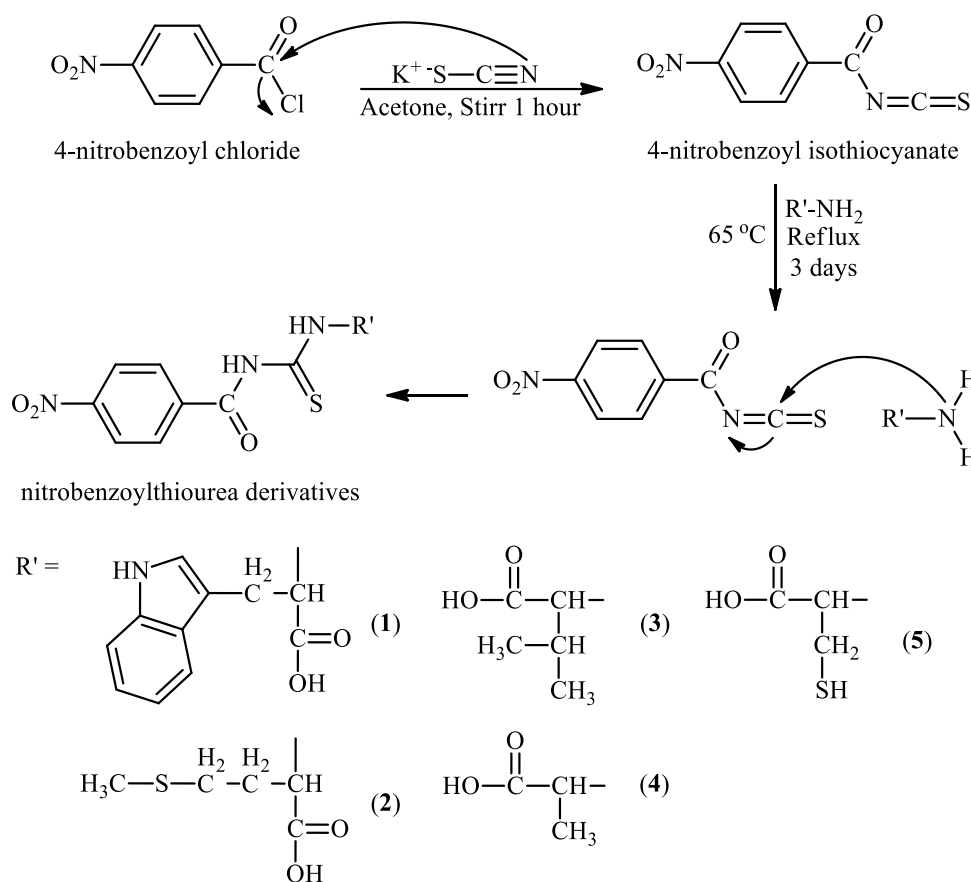
RESULTS & DISCUSSION

Thiourea Ligands

Thiourea ligands were synthesised *via* a sequence of nucleophilic substitution reactions, involving thiocyanate and isothiocyanate intermediates. Initially, the thiocyanate anion

(SCN⁻) serves as a nucleophile, attacking the carbonyl carbon of 4-nitrobenzoyl chloride. This interaction facilitates the displacement of the chloride ion, thereby yielding 4-nitrobenzoyl isothiocyanate. Subsequently, a primary amine (R'-NH₂), which is the amino acid series engages in a nucleophilic attack on the electrophilic carbon of the isothiocyanate group (N=C=S) within the 4-nitrobenzoyl

isothiocyanate. This nucleophilic addition leads to the formation of a thiourea linkage (-NH-C=S), resulting in the corresponding nitrobenzoylthiourea derivatives. Thiourea derivatives (**1-5**) were successfully synthesized with the percentage yields of 81.40%, 81.11%, 89.51%, 79.5% and 82.15% respectively. The synthesis pathway of the thiourea ligand was depicted in scheme 1.



Scheme 1: Synthesis pathway of thiourea ligand (**1-5**)

All synthesised compounds were characterised using CHNS elemental analysis, FT-IR, ¹H and ¹³C NMR spectroscopy. The elemental analysis data of ligand **1-5** are shown in Table 1. The FT-IR spectra showed the successful formation of thiourea compounds through the absence of ν(NCS) group at 2000 cm⁻¹ to 2400 cm⁻¹ and the presence of expected absorption at 3100 cm⁻¹ to 3400 cm⁻¹ attributed to ν(NH) band (Fakhar *et al.*, 2018). This result from the conversion of (NCS) to (NH) which also indicates that all (NCS) has reacted with the amino acid. For ligands (**1-5**), the ν(C=O) stretching of carboxylic were observed at 1722 cm⁻¹ to 1709 cm⁻¹. Apart from that, distinctive peaks were also observed between 1681 cm⁻¹ to

1659 cm⁻¹ that attributed to the presence of ν(C=O) of amide group of ligands (**1-5**) respectively. These distinctive peak apparently were decreased in frequency compared to ordinary amides absorption range due to the formation of intramolecular hydrogen bond interaction (Khairul *et al.*, 2016) between the hydrogen atom of thio-amide group (H-N-C=S) and the oxygen atom of carbonyl group (C=O) (Fakhar *et al.*, 2018). Moreover, the C=O group (benzoyl) occurred at 1681 to 1659 cm⁻¹ which was lower than the usual carbonyl group at 1760-1685 cm⁻¹, is due to the conjugation towards the benzene ring and the hydrogen bond formation with NH (Li *et al.*, 2010). Table 2 summarises the important bands observed in the FTIR

spectra of nitrobenzoylthiourea derivatives (**1-5**).

The ^1H NMR and ^{13}C NMR spectroscopic analysis was performed for all nitrobenzoylthiourea ligands (**1-5**). For ^1H NMR two (NH) peaks can be observed which represent resonance of (CONH) and (CSNH). The proton resonance of (CONH) in which the proton bonded to carbonyl group can be noticed at higher chemical shift compared to the resonance of (CSNH) in which the proton is bonded to thiocarbonyl group. This might be due to electron withdrawing effect of oxygen and sulphur (Hassan *et al.*, 2011), and the presence of deshielding aromatic ring near (CONH) group making it more deshielded and exist downfield at higher frequency compared to proton of (CSNH). The chemical shifts of the two (N-H) signals were distinct, owing to the existence and

influence of the electron withdrawing group and intramolecular hydrogen bond in the molecule (Saeed *et al.*, 2010; Raheel *et al.*, 2016). Distinctive multiple resonances at δ_{H} 8.28-8.09 ppm were observed due to the presence of proton of the aromatic group. Apart from that, the formation of thiourea ligands were confirmed by the appearance of carbon peak signals. The carbon peaks of (CONH) were more deshielded and present at the most downfield frequency followed by the carbon of (COOH) and (CSNH) due to the higher electronegativity value of oxygen compared to sulphur atom. The spectra of ^{13}C NMR exhibited carbonyl (C=O) at δ_{C} 172.4-181.0 ppm and δ_{C} 166.3-173.3 ppm corresponding to (CONH) and (C=OO) respectively. The successful formation of thiourea compound was also confirmed by the signal at δ_{C} 149.9-167.8 ppm represents (CSNH) thiocarbonyl.

Table 1. CHNS elemental analysis of nitrobenzoylthiourea derivatives 1-5

Thiourea	Molecular Formula	Molecular Weight	Measured value (Theoretical Value)			
			% Carbon	% Hydrogen	% Nitrogen	% Sulphur
1	$\text{C}_{19}\text{H}_{16}\text{N}_4\text{O}_5\text{S}$	414.42	55.72(55.33)	4.18(3.91)	13.87(13.58)	6.51(7.77)
2	$\text{C}_{13}\text{H}_{15}\text{N}_3\text{O}_5\text{S}_2$	357.41	43.71(43.69)	4.22(4.23)	11.82(11.76)	17.76(17.94)
3	$\text{C}_{13}\text{H}_{15}\text{N}_3\text{O}_5\text{S}$	325.34	48.16(47.99)	4.73(4.65)	12.97(12.92)	8.26(9.86)
4	$\text{C}_{11}\text{H}_{11}\text{N}_3\text{O}_5\text{S}$	297.29	44.84(44.44)	3.97(3.73)	14.53(14.13)	8.68(10.79)
5	$\text{C}_{11}\text{H}_{11}\text{N}_3\text{O}_5\text{S}_2$	329.35	40.43(40.11)	3.57(3.37)	14.07(12.76)	16.49(19.47)

Table 2. Important bands observed in the FTIR spectra of nitrobenzoylthiourea derivatives 1-5

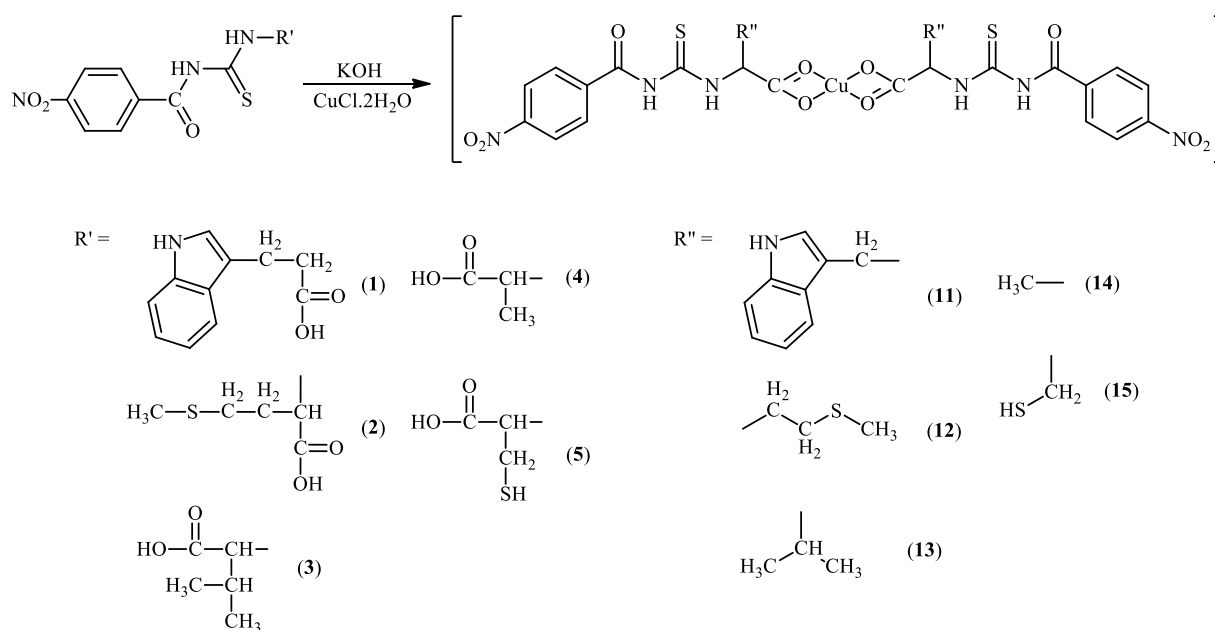
Thiourea ligand	$\nu(\text{NH})$	$\nu(\text{C=O})$ carboxylic	$\nu(\text{C=O})$ amide	$\nu(\text{C=C})$ aromatic	$\nu(\text{C=S})$	$\nu(\text{CN})$
1	3412	1716	1674	1514	854	1159
2	3218	1722	1681	1508	853	1156
3	3237	1716	1672	1521	854	1163
4	3281	1709	1659	1532	847	1167
5	3113	1716	1668	1519	848	1157

Copper(II) Complexes of Thiourea

Copper(II) complexes were synthesised through a process that involved the deprotonation of the

carboxylic acid group present in the nitrobenzoylthiourea ligands. This deprotonation step generates a carboxylate anion, which then facilitates the coordination of copper(II) ions to form stable copper(II) thiourea complexes *via* chelation. Copper(II) complexes (**6-10**) were successfully synthesised with satisfactory percentage yield of 68.7%, 57.6%,

65.1%, 55.2% and 76.2%, respectively. Scheme 2 illustrated the synthesis pathway of copper(II) complexes (**6-10**).



Scheme 2: Synthesis pathway of copper(II) complexes of thiourea (6-10)

The CHNS elemental analysis data of copper(II) complexes (**6-10**) are in good agreement with the theoretical value as showed in Table 3. FTIR analysis of copper(II) complexes (**6-10**) was conducted to demonstrate significant changes in the functional group stretching vibrations upon complexation, as evidenced by the shifting of the designated peaks and intensities in their spectra. These changes confirm the coordination sites of ligands (**1-5**) to the metal ions in the complex. In addition, the shifts experienced by the $\nu(\text{C}=\text{O})$ carboxylic ($1709\text{--}1722\text{ cm}^{-1}$) towards lower region ($1671\text{--}1703\text{ cm}^{-1}$) in the IR spectrum of (**6-10**) possibly indicate the coordination to the Cu(II) metal centre through the carboxylate binding site to form the thiourea complexes. The shifting of the peak towards the lower region was due to the deprotonation that induced the delocalisation of the electron and conforming the coordination through oxygen (Mishra *et al.*, 2012). In addition, the decrease in shifting frequency observed in complex (**10**), compared to its free ligand, suggests a reduction in the bond order of

the $\text{C}=\text{O}$ bond upon coordination to the copper(II) metal (Welch *et al.*, 2022). The carbonyl of $\nu(\text{C}=\text{O})$ of amide group showed slight chemical shift from 1659 cm^{-1} to 1681 cm^{-1} in the free ligand to 1651 cm^{-1} to 1682 cm^{-1} of metal complexes. In addition, there was very little to no variable shift of $\nu(\text{C}=\text{S})$ and $\nu(\text{C}-\text{N})$ in the complex in comparison to the free ligands. This observation suggests that the $(\text{C}=\text{S})$ group does not form any coordinate covalent bond with the metal ions. This interpretation is consistent with the unchanged spectral features between the free ligands and the complex, indicating that the chemical environment around these functional groups remains largely unaffected by metal coordination. The FTIR stretching vibration values of copper(II) complexes (**6-10**) were shown in Table 4. Due to the paramagnetic nature of copper(II) complexes, ^1H and ^{13}C NMR experiments was not performed on all of the copper(II) complexes. The paramagnetic properties of the complexes could cause severe broadening of NMR signals, making NMR an ineffective method for their analysis.

Table 3. CHNS elemental analysis of thiourea complex 6-10

Complex	Molecular Formula	Molecular Weight (g/mol)	Measured value (Theoretical Value)
---------	-------------------	--------------------------	------------------------------------

			% C	% H	% N	% S
6	C ₃₈ H ₃₂ CuN ₈ O ₁₀ S ₂	888.38	43.16 (43.53)	3.85 (4.61)	10.62 (10.69)	6.61 (6.12)
7	C ₂₆ H ₃₀ CuN ₆ O ₁₀ S ₄	778.36	37.25 (37.61)	3.73 (4.13)	10.52 (10.12)	15.61 (15.45)
8	C ₂₆ H ₂₈ CuN ₆ O ₁₀ S ₂	712.21	48.73 (38.92)	4.30 (4.77)	10.85 (10.48)	9.21 (7.99)
9	C ₂₂ H ₂₀ CuN ₆ O ₁₀ S ₂	656.10	34.30 (34.58)	3.90 (4.22)	11.04 (11.00)	9.89 (8.39)
10	C ₂₂ H ₂₀ CuN ₆ O ₁₀ S ₄	720.23	36.64 (36.69)	3.08 (2.80)	12.26 (11.67)	12.75 (17.81)

Table 4. FTIR spectrum of thiourea complex 6-10

Thiourea complexes	v(NH)	v(C=O) amide	v(C=C) aromatic	v(C=S)	v(CN)
6	3170	1681	1520	853	1171
7	2986	1682	1523	854	1169
8	2964	1679	1519	853	1166
9	3116	1671	1519	854	1170
10	3072	1651	1523	851	1168

Antibacterial Activity

The antibacterial activity of all produced compounds at different concentrations (150 ppm, 250 ppm, 500 ppm, and 1000 ppm) was determined using the disc diffusion method. The compounds (**1-10**) were tested against several bacteria, including *Staphylococcus aureus*, *Bacillus cereus*, *Listeria monocytogenes*, *Escherichia coli*, *Klebsiella pneumoniae*, and *Pseudomonas aeruginosa*. Standard antibiotics were used as positive controls, and DMSO served as the negative control (Ngaini & Mortadza, 2019). The results were classified as mild (6-13 mm) or moderate (14-16 mm) based on the inhibition zones (Halim & Ngaini, 2017). The antibacterial activity of thiourea compounds (**1-10**) against gram-positive bacteria is summarized in Table 5.

Notably, all ligands showed little bactericidal activity against gram-positive bacteria at concentrations below 500 ppm. This low activity

could be due to steric hindrance caused by bulky groups, such as the tryptophan and nitrobenzoyl groups in ligand **1**, which block the interaction between the compound's active sites and the bacterial receptor sites (Smith, 2017; Fakhar *et al.*, 2018). As lipophilicity is a key factor in a compound's bioactivity (Arslan *et al.*, 2009), steric hindrance decreases lipophilicity, making it harder for the compound to penetrate bacterial cell membranes, thus reducing the antibacterial activity (Ngaini *et al.*, 2012).

However, at both 500 ppm and 1000 ppm, ligands **1** and **2** showed mild antibacterial activity against gram-positive bacteria (*B. cereus*, *L. monocytogenes*, and *S. aureus*). Ligand **2**'s activity may be due to the longer aliphatic chain in its structure, which increases biological activity by enhancing lipophilicity (Liang *et al.*, 2018; Fatima *et al.*, 2017).

The incorporation of copper(II) into the thiourea complexes (**6-10**) led to more effective

inhibition of gram-positive bacteria. At both 500 ppm and 1000 ppm, all complexes showed antibacterial activity, particularly against *S. aureus*, with complex **8** showing the highest activity. The copper(II) complexes also significantly increased antibacterial activity of complex **9** and **10** against *B. cereus* compared to their free ligands **4** and **5**. This improved activity could possibly be due to the effect of chelation, which reduces metal ion polarity and increases lipophilicity, allowing better penetration through bacterial cell membranes (Sumrra *et al.*, 2014; Ramesh *et al.*, 2016).

For gram-negative bacteria, the thiourea ligands (**1-5**) showed no activity at concentration below 500 ppm, except for ligand **4**, which had notable activity against *K. pneumoniae* starting at 150 ppm. This could possibly be due to the smaller size of alanine that enhance the antibacterial activity, which is in agreement with the data reported by Madabhushi *et al.* (2014). Ligands **2**, **3**, and **5** showed only mild activity at 500 ppm and 1000 ppm. Copper(II) complexes (**6-10**), however, showed mild to moderate

activity against gram-negative bacteria, with complex **9** being the most active at concentrations below 500 ppm. This further demonstrates the role of metal ions in enhancing antibacterial effects (Boros *et al.*, 2020; Claudel *et al.*, 2020). The metal-ligand complex increases lipophilicity, helping the complex penetrate bacterial cell membranes and deactivate bacteria (Liang *et al.*, 2018; Arendsen *et al.*, 2019). The antibacterial activity of the thiourea compounds (**1-10**) against gram-negative bacteria is shown in Table 6.

Overall, metal complexes exhibited better antibacterial activity than free ligands, especially against gram-positive bacteria, which are generally more susceptible to antibacterial agents due to their cell wall structure (Mukherjee *et al.*, 2017). Complex **10** was the most effective against gram-positive bacteria, while complex **9** showed the highest inhibition against gram-negative bacteria. The inhibition zones for the thiourea ligands (**1-5**) and copper(II) complexes (**6-10**) are shown in Figures 1- 4.

Table 5. Zone of inhibition (mm) of thiourea compounds (1-10) on gram positive bacteria

Concentration (ppm)	Zone of Inhibition (mm)											
	<i>S. aureus</i>				<i>B. cereus</i>				<i>L. monocytogenes</i>			
	150	250	500	1000	150	250	500	1000	150	250	500	1000
Compound												
1	-	-	-	-	-	-	8	9	-	-	-	-
2	-	-	10	10	-	-	-	-	-	-	7.5	9
3	-	-	-	-	-	-	-	-	-	-	-	-
4	-	-	-	-	-	-	-	-	-	-	-	-
5	-	-	-	-	-	-	-	-	-	-	-	-
6	-	-	7	11	-	-	-	-	-	-	-	-
7	-	-	7	10	-	-	-	-	7.5	7.5	7.5	7.5
8	-	-	13	15	-	-	-	-	-	-	-	-
9	-	-	9	15	-	-	9.5	10	-	-	-	-
10	9.5	9.5	9.5	10	-	-	8	9.5	-	-	-	-

DMSO (-): 6.5 mm

Standard antibiotic (+):

Penicillin = 17 mm

Vancomycin = 15 mm

Ampicillin = 19 mm

*Note: (-) = No activity

Table 6. Zone of inhibition (mm) of synthesized compound on gram negative bacteria

	Zone of Inhibition (mm)		
	<i>E. coli</i>	<i>K. pneumoniae</i>	<i>P. aeruginosa</i>

Compound	Concentration (ppm)				Concentration (ppm)				Concentration (ppm)			
	150	250	500	1000	150	250	500	1000	150	250	500	1000
1	-	-	-	-	-	-	-	-	-	-	-	-
2	-	-	-	7	-	-	8	8	-	-	9	12
3	-	-	-	-	-	-	7	7	-	-	-	-
4	-	-	-	-	12	13	13	14	-	-	-	-
5	-	-	-	-	-	-	10	11	-	-	-	-
6	-	-	8	9.5	-	-	-	-	-	-	-	-
7	7	7	7	9	-	-	8	8	-	-	-	7.5
8	8	8	8	8	-	-	12	16	-	-	-	-
9	7	7.5	8.5	9	7	7.5	8.5	9	-	8	8	8
10	-	-	7.5	7.5	-	-	-	7	-	-	8	9

DMSO (-): 6.5 mm
 Standard antibiotic (+):
 Tetracycline = 19 mm
 Cefazidime = 17 mm
 Imipenem = 17 mm

*Note: (-) = No activity

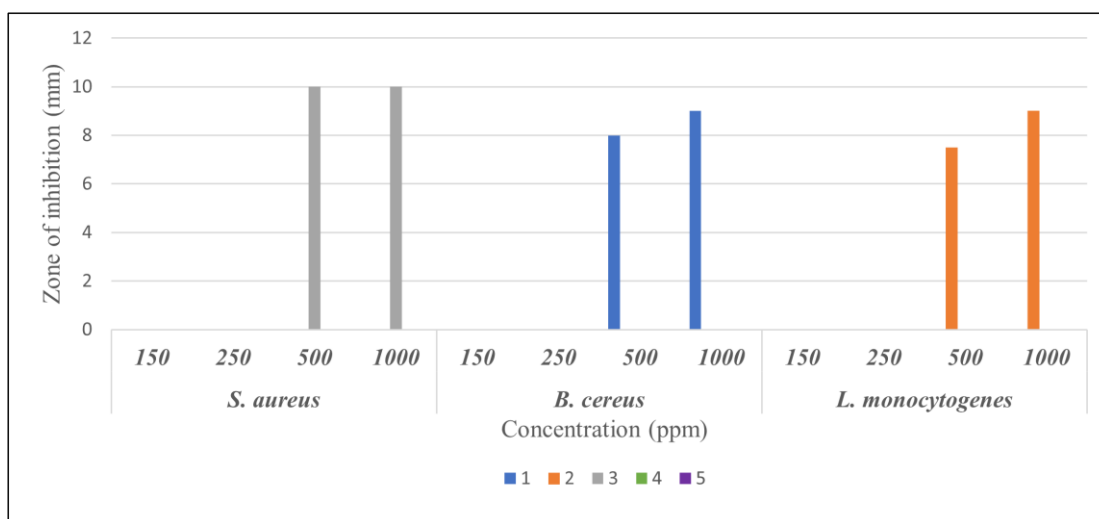


Figure 1. The zone of inhibition (mm) of thiourea ligand (1-5) on gram-positive bacteria

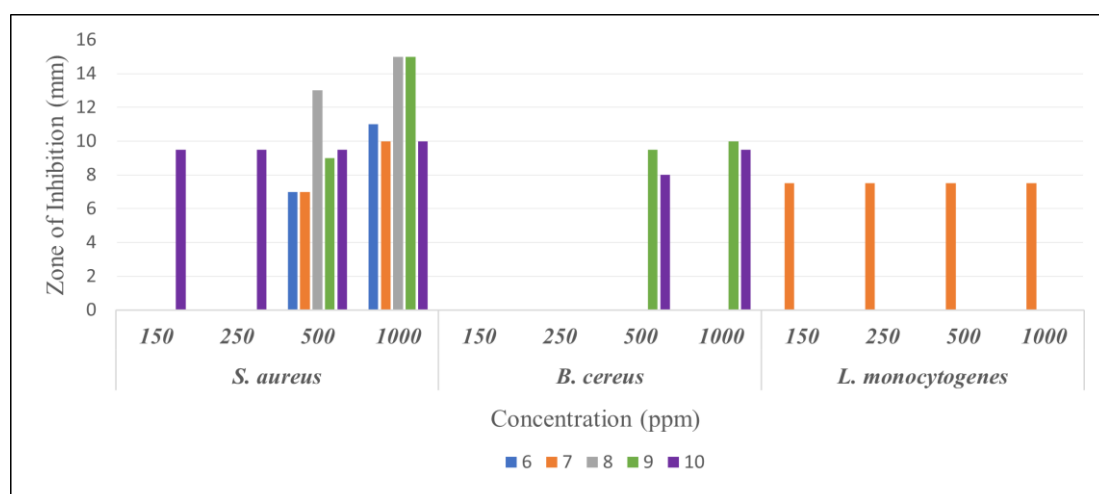


Figure 2. The zone of inhibition (mm) of thiourea copper(II) complex (6-10) on gram-positive bacteria

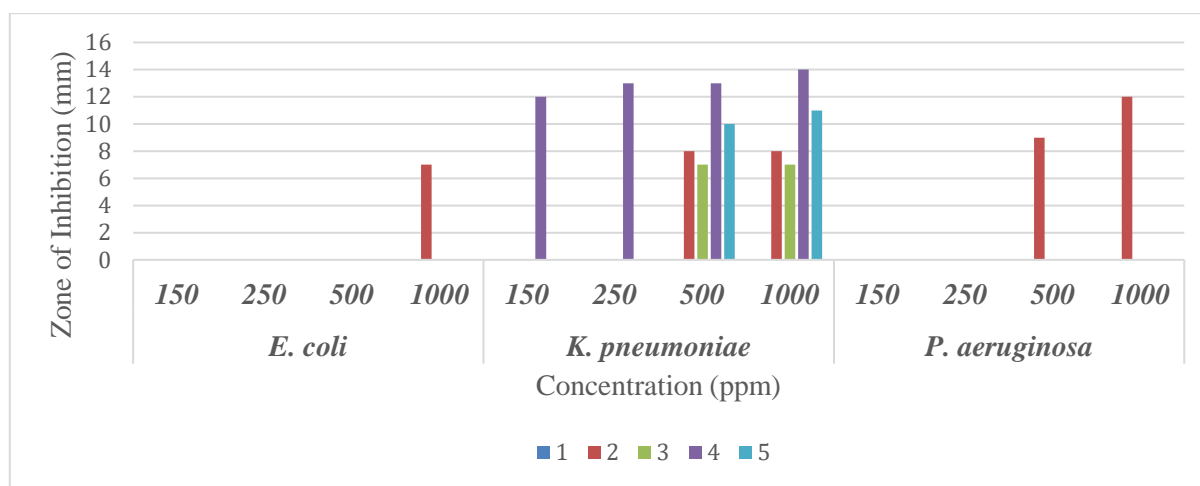


Figure 3. The zone of inhibition (mm) of thiourea ligand (1-5) on gram-negative bacteria

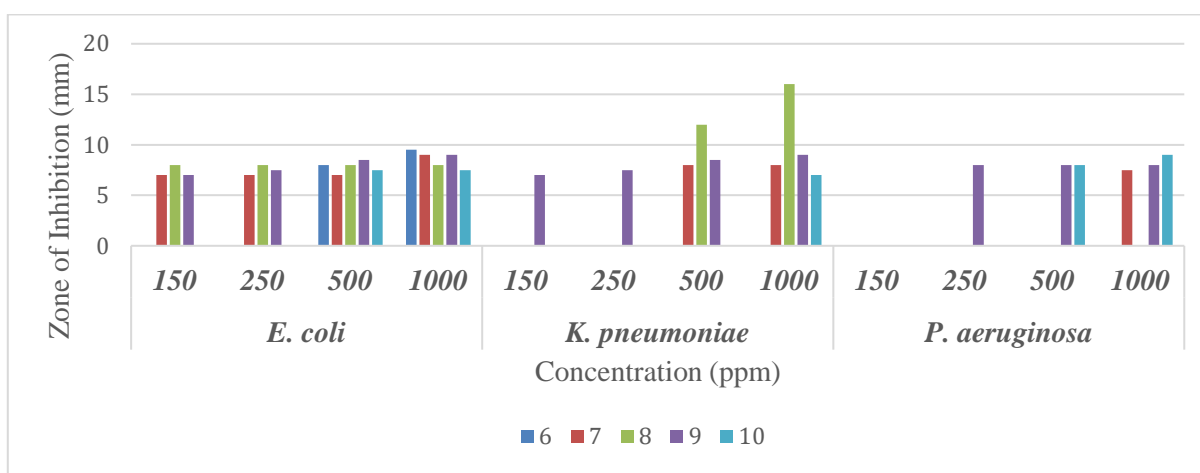


Figure 4. The zone of inhibition (mm) of thiourea copper(II) complex (6-10) on gram-negative bacteria

Molecular Docking Study

Molecular docking was employed to predict the interactions between synthesised compounds (ligand and complexes) and targeted proteins at the atomic level, aiding in understanding the mode of action in antibacterial activity (Echeverria *et al.*, 2017). In this study, we focused on the compounds with the inhibition zones of 10 mm or greater from the antibacterial studies to prioritise candidates with the highest antibacterial potency. The findings from the docking studies were used to provide an insight on what are the possible factors that contribute to the antibacterial properties of the selected compounds, such as the binding affinity (docking score), interaction between the compounds and the proteins (e.g hydrogen bonds, hydrophobic interaction etc) or how well the compounds fit into the binding pockets. The targeted proteins for this study were PDB ID

4XWA (*S. aureus*), PDB ID 7ci4 (*P. aeruginosa*), PDB ID 5xun (*K. pneumoniae*) and PDB ID 5BCA (*B. cereus*), which are highly crucial for the survival of the named bacteria (Mahone & Goley., 2020; Bush & Bradford., 2016; Zeng & Lin., 2013; Ambade *et al.*, 2023).

For free ligand **2**, the obtained binding energy against *S. aureus* and *P. aeruginosa*, were -7.7 kcal/mol and -6.7 kcal/mol respectively, while the obtained binding energy for free ligand **4** against *K. pneumoniae* was -6.7 kcal/mol. The binding energies obtained were consistent with the mild antibacterial activity of these compounds against the respected bacteria. Comparison was also made with the free amino acids that present in free ligand **2** which is methionine against both *S. aureus* and *P. aeruginosa*, which results in the binding energy of -4.4 kcal/mol and -3.8 kcal/mol respectively. Likewise, the same experiment was conducted

on alanine, an amino acid block of free ligand **4** which resulted in the binding energy of -3.9 kcal/mol. These data shows that the presence of thiourea moiety in the synthesised compounds, **2** and **4** could possibly result in the formation of more hydrogen bonds that contributed to the enhanced binding affinity of the synthesised compounds with the targeted protein receptors (Ngaini *et al.*, 2020). An illustration of the molecular docking for the interactions of the ligands and the receptors is depicted in Figure 5-7 while the molecular binding pocket of ligand **2** docked with *S. aureus* and *P. aeruginosa* as well as ligand **4** docked with *K. pneumoniae* is shown in Figure 8.

On the other hand, the copper(II) complexes (**6-10**) were shown to have stronger binding affinity to the targeted proteins with lower binding energy compared to the free ligands **2** and **4**. Of all the copper(II) complexes studied, complex **6** showed the strongest binding affinity with the lowest binding energies of -10.4 kcal/mol, followed by complex **9** (-9.8 kcal/mol), **8** (-9.4 kcal/mol), **10** (-9.3 kcal/mol) and **7** (-9.0 kcal/mol) (Table 8). The molecular

binding pocket of *S. aureus* docked with complex **6-10** is illustrated in Figure 9. The 3D Pymol Modelling shows that complex **6** formed ten hydrogen bonds with nine important amino acid residues of protein PDB ID 4XWA (*S. aureus*), particularly between the metal-bound oxygen with the -NH groups of SER-175 in the enzyme's binding pocket that could possibly be the key interaction that contributed to the inhibitory activity. These interactions, especially with polar substituents like -NO₂, -NH, and C=O groups, can enhance the binding stability and are likely responsible for the observed biological activity (Maalik *et al.*, 2019; Souza *et al.*, 2021). The 3D Pymol Modelling for other complexes in shown in Table 9 to 11. Nevertheless, there was no π - π interaction observed between the aromatic ring of the inhibitor and bacteria, although there are some aromatic rings present in the compounds. Although this data provides some insights to the inhibition of the bacteria, it is still not conclusive and have some limitations and more thorough investigation should be made particularly on the inhibition mechanism of the synthesised compounds.

Table 7. The molecular docking results for thiourea ligand **2**, **4** and its respected antibiotic with *S. aureus* (PDB entry: 4xwa), *P. aeruginosa* (PDB entry: 7ci4) and *K. pneumoniae* (PDB entry: 5xun) including the binding affinity and important amino acid residues of proteins that interact with the compounds

Ligand	PDB entry	Binding score value (kcal/mol)	Important Residue
2	4xwa	-7.7	Gly12, Ser13, Gly14, Lys15 and Thr16
2	7ci4	-6.7	Glu55 and Arg272
4	5xun	-6.9	Thr64, Thr93 and Tyr86
Methionine	4xwa	-4.4	Thr16, Gly14, Ser13 and Cys15
Methionine	7ci4	-3.8	Asn251 and Asp89
Alanine	5xun	-3.9	Arg96 and Ser66

Table 8. The molecular docking results for thiourea complex **6**, **7**, **8**, **9** and **10** with *S. aureus* (PDB entry: 4xwa), *B. cereus* (PDB entry: 5bca) and *K. pneumoniae* (PDB entry: 5xun) including the binding affinity score and important amino acid residues of proteins that interact with the compounds

Complex	PDB entry	Binding score value (kcal/mol)	Important Residue
6	4xwa	-10.4	Ser180, Arg48, Ser 175, Glu11, Thr16, Lys15, Gly14, Ser13 and Gly12
7	4xwa	-9.0	Thr16, Lys15, Ser13, Gly12, Glu11 and Ser175
8	4xwa	-9.4	Ser180, Arg48, Ser175, Arg92 and Lys15
9	4xwa	-9.8	Ser180, Asn173, Glu11, Lys15, Ser175 and Gly176
10	4xwa	-9.3	Ser180, Arg48, Ser 175, Glu11, Thr16, Lys15, Gly14 and Ser13
9	5bca	-8.3	Tyr343, Lys379, Arg380 and Ala444
8	5xun	-9.2	Cys69, Asn88, Ser66 and Arg96

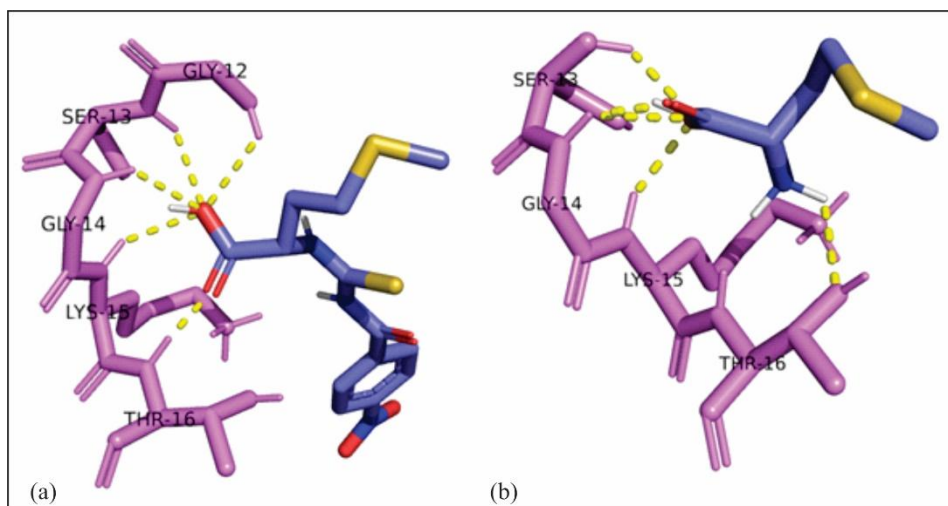


Figure 5. The 3D representation of the interactions for *S. aureus* (PDB ID: 4xwa) docked with (a) ligand 2 and (b) methionine.

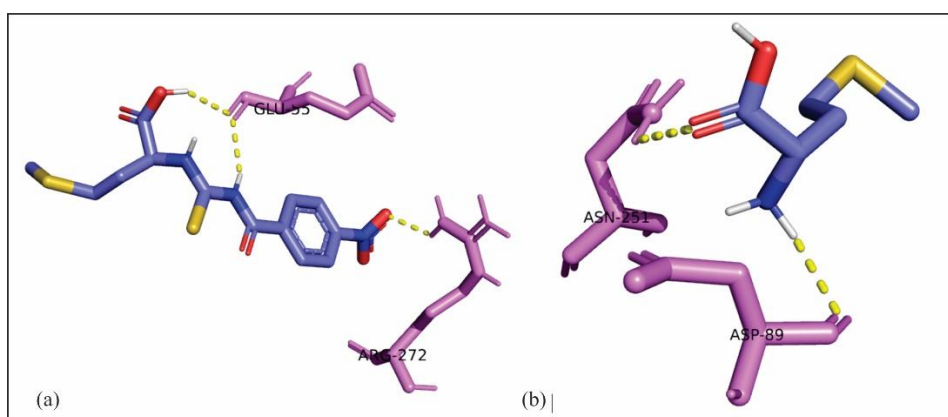


Figure 6. The 3D representation of the interactions for *P. aeruginosa* (PDB entry: 7ci4) docked with (a) ligand 2 and (b) methionine

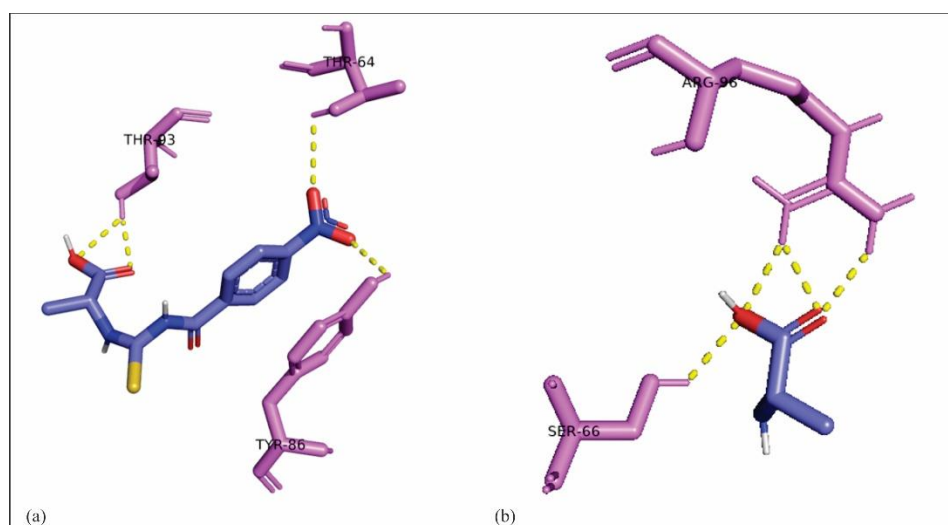


Figure 7. The 3D representation of the interactions for *K. pneumoniae* (PDB entry: 5xun) docked with (a) ligand 4 and (b) alanine

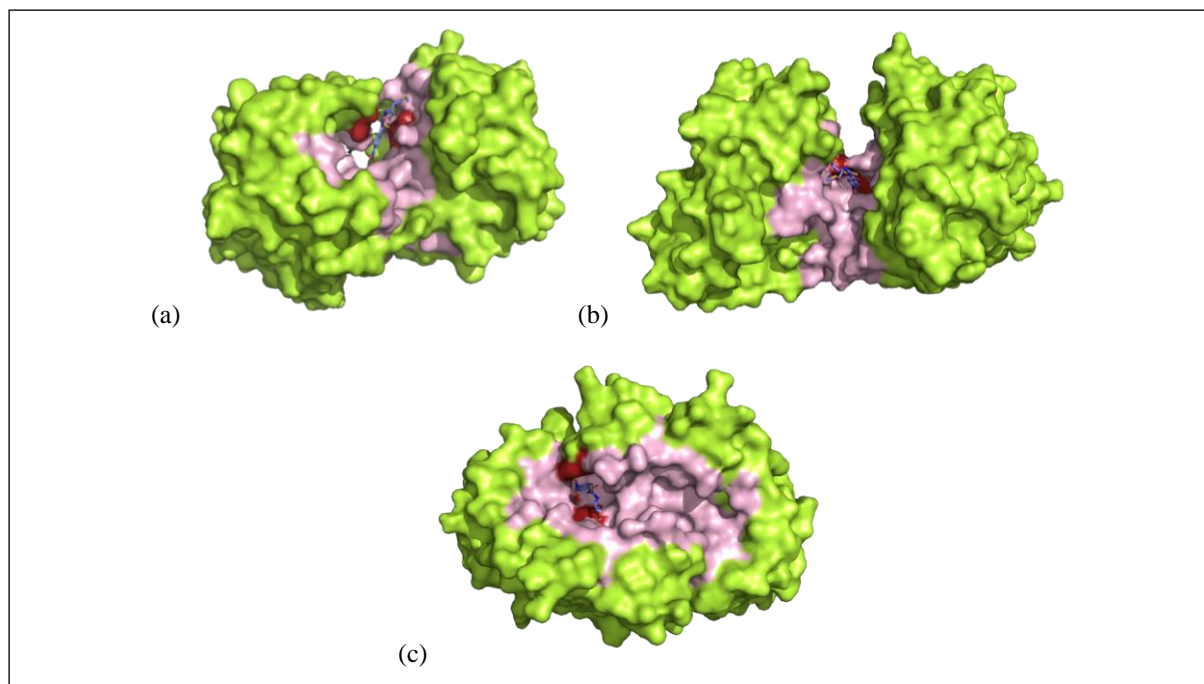


Figure 8. The molecular binding pocket of (a) ligand **2** docked with *S. aureus*, (b) ligand **2** docked with *P. aeruginosa* and (c) ligand **4** docked with *K. pneumoniae*

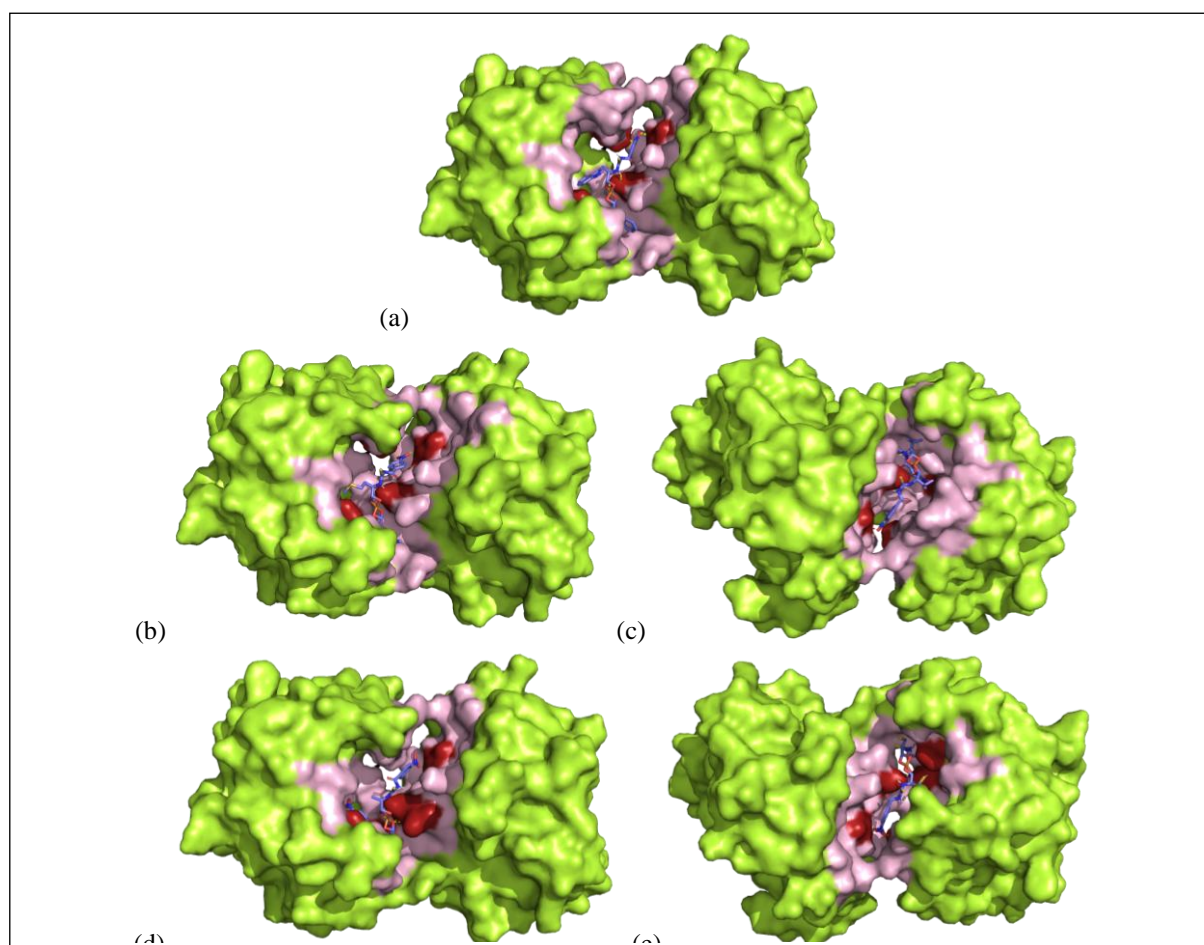


Figure 9. The molecular binding pocket of *S. aureus* docked with (a) complex **6**, (b) complex **7**, (c) complex **8**, (d) complex **9** and (e) complex **10**

Table 9. 3D docking illustration between complex 6, 7, 8, 9 and 10 against *S. aureus* (PDB entry: 4xwa)

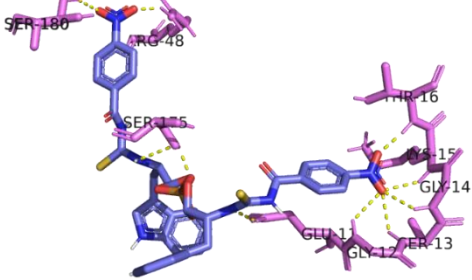
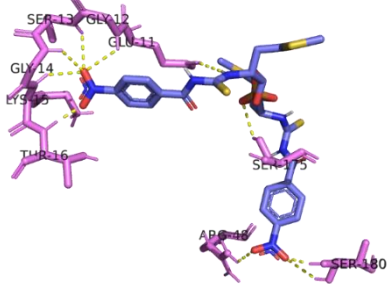
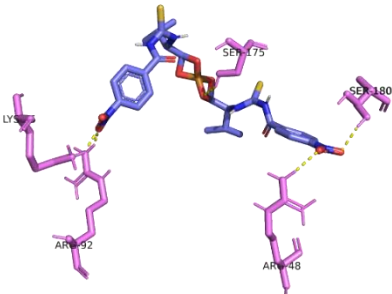
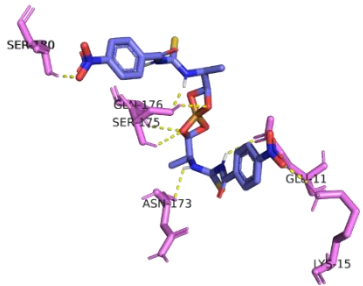
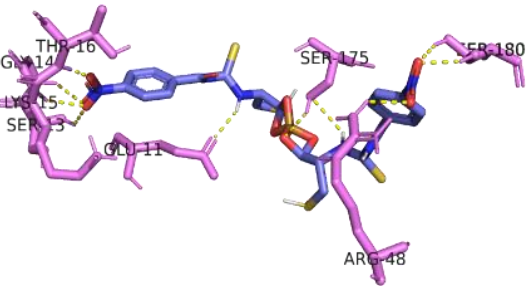
Complex	Binding poses (kcal/mol)	PyMol Modelling
6	-10.4	
7	-9.0	
8	-9.4	
9	-9.8	
10	-9.3	

Table 10. 3D docking illustration between complex 9 against *B. cereus* (PDB entry: 5bca)

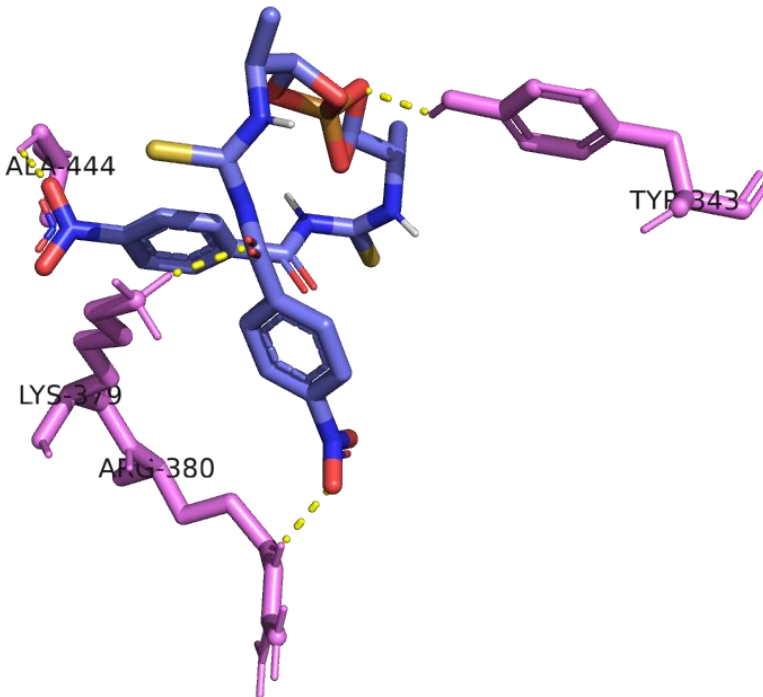
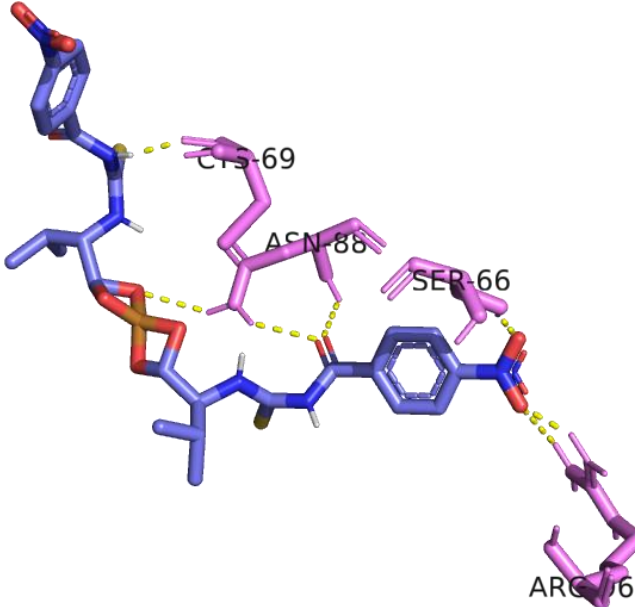
Complex	Binding poses (kcal/mol)	PyMol Modelling
9	-8.3	

Table 11. 3D docking illustration between complex 7 against *K. pneumoniae* (PDB entry: 5xun)

Complex	Binding poses (kcal/mol)	Pymol Modelling
7	-9.2	

CONCLUSION

In conclusion, nitrobenzoylthiourea derivatives were synthesised via one-pot reactions between nitrobenzoyl chloride, potassium thiocyanate and a series of chosen amino acids in acetone solvent under reflux conditions in moderate to high yields. On the other hand, Cu(II) complexes were prepared from the deprotonation of carboxylic acid moiety of the ligands and subsequent reaction with Cu(II) chloride with moderate yield. From the present studies, the incorporation of Cu(II) ions has enhanced the antibacterial activity of the free ligands which was measured based on the inhibition zones against both gram-positive and gram-negative bacteria. In the case of gram-positive bacteria, at 1000 ppm, complex **8** and **9** both inhibited the growth of *S. aureus* with 15 mm inhibition zones. Likewise, complex **8** also inhibited the growth of *K. pneumoniae* at the concentration of 1000 ppm with inhibition zone of 16 mm. Docking studies were conducted only on ligands and complexes that shown 10 mm and greater inhibition zone to provide some insights on what factors that could possibly contributed to the antibacterial activity. Complexes **6-10** have shown good binding energies between -10.4 kcal/mol to -9.0 kcal/mol and these findings correlates to the enhanced antibacterial activity of the copper(II) complexes synthesised.

The present study has several limitations. First, the scope of the research is confined to the molecular docking of four specific protein structures (PDB IDs: 4xwa, 7ci4, 5xun and 5bca), which may not represent the full range of possible interactions. Additionally, the accuracy of the docking predictions is inherently limited by the resolution of the protein structures used and the constraints of the computational algorithms. Furthermore, this study relies on available crystallographic data, which may not fully capture dynamic conformational changes in proteins. Consequently, experimental validation is necessary to confirm the predicted interactions. Future studies could extend these findings by including more diverse protein-ligand complexes and employing enhanced molecular dynamics simulations.

Supporting Materials Summary

The characterization data FTIR spectrometer, ¹H and ¹³C NMR spectroscopy on each of

compound for this article can be accessed as supplementary data.

ACKNOWLEDGEMENT

The work is financially supported through E07/SpMYRA/1713/2018. We are thankful to Universiti Malaysia Sarawak for the Zamalah scholarship awarded to the first author.

REFERENCES

- Ambade, V., Ambade, S., Sharma V. & Sanas, P. (2023). Comparison between Amino Acid Profiling of Structural Proteins of earliest and recent omicron strain of SARS-CoV-2 and Nutritional Burden on COVID-19 patients. *Human Nutrition & Metabolism*, 34: 200220. DOI: <https://doi.org/10.1016/j.hnm.2023.200220>
- Arendsen, L.P., Thakar, R. & Sultan, A. H. (2019). The use of copper as an antimicrobial agent in health care, including obstetrics and gynecology. *Clinical Microbiology Reviews*, 32(4): 25-18. DOI: 10.1128/CMR.00125-18
- Arslan, H., Duran, N., Borekci, G., Ozer, C.K. & Akbay, C. (2009). Antimicrobial activity of some thiourea derivatives and their nickel and copper complexes. *Molecules*, 14(1): 519–527. DOI: 10.3390/molecules14010519
- Azócar, M.I., Gómez, G., Levín, P., Paez, M., Muñoz, H. & Dinamarca, N. (2014). Review: Antibacterial behavior of carboxylate silver(I) complexes. *Journal of Coordination Chemistry*, 67: 3840–3853. DOI: 10.3390/molecules23071629
- Boros, E., Dyson, P.J. & Gasser, G. (2020). Classification of metal-based drugs according to their mechanisms of action. *Chemistry*, 6(1): 41–60. DOI: 10.1016/j.chempr.2019.10.013
- Bush, K., and Bradford, P. A. (2016). β -Lactams and β -lactamase inhibitors: an overview. *Cold Spring Harb. Perspect. Med.* 6: 295–306. DOI: 10.1101/cshperspect.a025247
- Claudel, M., Schwarte, J.V. & Fromm, K.M. (2020). New antimicrobial strategies based on metal complexes. *Chemistry*, 2(4): 849–899. DOI: <https://doi.org/10.3390/chemistry2040056>
- Drzewiecka-Antonik, A., Rejmak, P., Klepka, M., Wolska, A., Chrzanowska, A. & Struga, M. (2020). Structure and anticancer activity of Cu(II)

- complexes with (bromophenyl)thiourea moiety attached to the polycyclic imide. *Journal of Inorganic Biochemistry*, 212(6): 8-16. DOI: <https://doi.org/10.1016/j.jinorgbio.2020.111234>
- Echeverría, J., Urzúa, A., Sanhueza, L. & Wilkens, M. (2017). Enhanced antibacterial activity of ent-labdane derivatives of salvic acid (7 α -hydroxy-8(17)-ent-labden-15-oic acid): effect of lipophilicity and the hydrogen bonding role in bacterial membrane interaction. *Molecules*, 22(7): 1-19. DOI: 10.3390/molecules22071039
- Fair, R. J. & Tor, Y. (2014). Antibiotics and bacterial resistance in the 21st century. *Perspectives in Medicinal Chemistry*, 6: 25–64. DOI: <https://doi.org/10.4137/pmc.s14459>
- Fakhar, I., Hussien, N.J., Sapari, S., Bloh, A.H., Yusoff, S.F.M., Hasbullah, S.A., Yamin, B.M., Mutalib, S.A., Shihab, M.S. & Yousif, E. (2018). Synthesis, x-ray diffraction, theoretical and antibacterial studies of bis-thiourea secondary amine. *Journal of Molecular Structure*, 1159: 96–102. DOI: <https://doi.org/10.1016/j.molstruc.2018.01.032>
- Fatima, T., Haque, R.A., Razali, M.R., Ahmad, A., Asif, M., Khadeer Ahamed, M.B. & Abdul Majid, A.M.S. (2017). Effect of lipophilicity of wingtip groups on the anticancer potential of mono N-heterocyclic carbene silver(I) complexes: Synthesis, crystal structures and in vitro anticancer study. *Applied Organometallic Chemistry*, 31(10): 1–13. DOI: <https://doi.org/10.1002/aoc.3735>
- Halim, A.A.N. & Ngaini, Z. (2017). Synthesis and characterization of halogenated bis(acylthiourea) derivatives and their antibacterial activities. *Phosphorus, Sulfur and Silicon and the Related Elements*, 192(9): 1012–1017. DOI: <https://doi.org/10.1080/10426507.2017.1315421>
- Halim, A.N.A. & Ngaini, Z. (2016). Synthesis and bacteriostatic activities of bis(Thiourea) derivatives with variable chain length. *Journal of Chemistry*, 2016(3): 1-7. DOI: <https://doi.org/10.1155/2016/2739832>
- Hassan, I.N., Yamin, B.M., Daud, W.R.W. & Kassim, M. B. (2011). Synthesis, spectral characterisation and crystal structural of 1-(2-morpholinoethyl)-3-(3-phenylacryloyl)thiourea. *International Journal of Physical Sciences*, 6(35): 7898–7903. DOI: <https://doi.org/10.5897/IJPS11.1458>
- Idrees, M., Mohammad, A.R., Karodia, N. & Rahman, A. (2020). Multimodal role of amino acids in microbial control and drug development. *Antibiotics*, 9(6): 1–23. DOI: <https://doi.org/10.3390/antibiotics9060330>
- Ikokoh, P.P.A., Onigbanjo, H.O., Adedirin, O., Akolade, J.O., Uzo, A. & Fagbohun, A. (2015). Synthesis and antimicrobial activities of copper(I) thiourea and silver(I) thiourea. *Open Journal of Research*, 2(2): 086-091.
- Khairul, W.M., Tukimin, N. & Rahamathullah, R. (2016). Synthesis, characterization and electrical properties of N-([4-(aminophenylethynyl)toluene]-N'-(cinnamoyl)thiourea (AECT) as single molecular conductive film. *Sains Malaysiana*, 45(5): 825–831.
- Li, Z., Zhang, Y. & Wang, Y. (2010). Synthesis and characterization of N-benzoyl-N' - carboxyalkyl substituted thiourea derivatives. *Phosphorus, Sulfur, and Silicon and the Related Elements*, 178(2): 293-297. DOI: <https://doi.org/10.1080/10426500307952>
- Liang, X., Luan, S., Yin, Z., He, M., He, C., Yin, L., Zou, Y., Yuan, Z., Li, L., Song, X., Lv, C. & Zhang, W. (2018). Recent advances in the medical use of silver complex. *European Journal of Medicinal Chemistry*, 157: 62–80. DOI: <https://doi.org/10.1016/j.ejmech.2018.07.057>
- Maalik, A., Rahim, H., Saleem, M., Fatima, N., Rauf, A., Wadood, A., Malik, M. I., Ahmed, A., Rafique, H., Zafar, M. N., Riaz, M., Rasheed, L. & Mumtaz, A. (2019). Synthesis, antimicrobial, antioxidant, cytotoxic, antiurease and molecular docking studies of N-(3-trifluoromethyl)benzoyl-N'-aryl thiourea derivatives. *Bioorganic Chemistry*, 88(5): 1-9. DOI: <https://doi.org/10.1016/j.bioorg.2019.102946>
- Madabhushi, S., Mallu, K., Vangipuram, V., Kurva, S., Poornachandra, Y. & Kumar, C. (2014). Synthesis of novel benzimidazole functionalized chiral thioureas and evaluation of their antibacterial and anticancer activities. *Bioorganic & Medicinal Chemistry Letters*, 24(20): 4822-4825. DOI: <https://doi.org/10.1016/j.bmcl.2014.08.064>
- Mahone C.R. & Goley E.D. Bacterial cell division at a glance. (2020). *J Cell Sci.* 133(7): jcs237057. DOI: <https://doi.org/10.1242/jcs.237057>

- Malik, M.A., Dar, O.A., Gull, P., Wani, M.Y. & Hashmi, A. A. (2018). Heterocyclic Schiff base transition metal complexes in antimicrobial and anticancer chemotherapy. *Medicinal Chemistry*, 9(3): 409–436. DOI: <https://doi.org/10.1039/c7md00526a>
- Mishra, A., Ninama, S., Sharma, P., Soni, N. & Awate, R. (2020). Synthesis, characterization, molecular docking and antimicrobial activity of copper(II) complexes of metronidazole and 1,10-phenanthroline. *Inorganica Chimica Acta*, 510: 6–11. DOI: <https://doi.org/10.1016/j.ica.2020.119744>
- Mohapatra, S.S., Dwibedy, S.K. & Padhy, I. (2021). Polymyxins, the last-resort antibiotics: Mode of action, resistance emergence, and potential solutions. *Journal of Biosciences*, 46(3): 1-18. DOI: <https://doi.org/10.1007/s12038-021-00209-8>
- Möhler, J.S., Kolmar, T., Synnatschke, K., Hergert, M., Wilson, L.A., Ramu, S., Elliott, A.G., Blaskovich, M.A.T., Sidjabat, H.E., Paterson, D. L., Schenk, G., Cooper, M. A. & Ziora, Z. M. (2017). Enhancement of antibiotic-activity through complexation with metal ions - combined ITC, NMR, enzymatic and biological studies. *Journal of Inorganic Biochemistry*, 167: 134–141. DOI: <https://doi.org/10.1016/j.jinorgbio.2016.11.028>
- Montero, D. A., Arellano, C., Pardo, M., Vera, R., Gálvez, R., Cifuentes, M., Berasain, M. A., Gómez, M., Ramírez, C. & Vidal, R. M. (2019). Antimicrobial properties of a novel copper-based composite coating with potential for use in healthcare facilities. *Antimicrobial Resistance and Infection Control*, 8(2019): 1-10. DOI: <https://doi.org/10.1186/s13756-018-0456-4>
- Mukherjee, I., Ghosh, A., Bhadury, P. & De, P. (2017). Side-chain amino acid-based cationic antibacterial polymers: investigating the morphological switching of a polymer-treated bacterial cell. *ACS Omega*, 2(4): 1633–1644. DOI: 10.1021/acsomega.7b00181
- Ngaini, Z., Mohd Arif, M.A., Hussain, H., Mei, E.S., Tang, D. & Kamaluddin, D. H. A. (2012). Synthesis and antibacterial activity of acetoxybenzoyl thioureas with aryl and amino acid side chains. *Phosphorus, Sulfur and Silicon and the Related Elements*, 187(1): 1–7. DOI: <https://doi.org/10.1080/10426507.2011.562398>
- Ngaini, Z. & Mortadza, N.A. (2019). Synthesis of halogenated azo-aspirin analogues from natural product derivatives as the potential antibacterial agents. *Natural Product Research*, 33(24): 3507–3514. DOI: <https://doi.org/10.1080/14786419.2018.1486310>
- Ngaini, Z., Rasin, F., Wan Zullkiplee, W.S.H. & Abd Halim, A. N. (2020). Synthesis and molecular design of mono aspirinate thiourea-azo hybrid molecules as potential antibacterial agents. *Phosphorus, Sulfur and Silicon and the Related Elements*, 196(3): 275–282. DOI: <https://doi.org/10.1080/10426507.2020.1828885>
- Ohammad, B. (2018). Synthesis, structure and spectroscopic properties of oxovanadium tris (3, 5-dimethylpyrazolyl) borate aroylthiourea complexes. *Sains Malaysiana*, 47(8): 1775–1785. DOI: <http://dx.doi.org/10.17576/jsm-2018-4708-16>
- Pingaew, R., Prachayasittikul, V., Anuwongcharoen, N., Prachayasittikul, S., Ruchirawat, S. & Prachayasittikul, V. (2018). Synthesis and molecular docking of N, N'-disubstituted thiourea derivatives as novel aromatase inhibitors. *Bioorganic Chemistry*, 79: 171-178.
- Raheel, A., Imtiaz-Ud-Din, Badshah, A., Rauf, M.K., Tahir, M.N., Khan, K.M., Hameed, A. & Andleeb, S. (2016). Amino acid linked bromobenzoyl thiourea derivatives: Syntheses, characterization and antimicrobial activities. *Journal of the Chemical Society of Pakistan*, 38(5): 959–964.
- Roche Allred, Z. D., Tai, H., Bretz, S. L. & Page, R. C. (2017). Using PyMOL to explore the effects of pH on noncovalent interactions between immunoglobulin g and protein a: a guided-inquiry biochemistry activity. *Biochemistry and Molecular Biology Education*, 45(6): 528–536. DOI: <https://doi.org/10.1002/bmb.21066>
- Ramesh, P., Revathi, M., H.A.A., Mohammeda, N. A. A., Siddappa, S., Reddy, P.M. & Pasha, C. (2016). Copper(II) complexes of new carboxamide ligands: synthesis, spectroscopic and antibacterial study. *International Journal of Advanced Research in Chemical Science*, 3(8): 1–8. DOI: <http://dx.doi.org/10.20431/2349-0403.0308001>
- Ronchetti, R., Moroni, G., Carotti, A., Gioiello, A. & Camaioni, E. (2021). Recent advances in urea and thiourea-containing compounds: focus on innovative approaches in medicinal chemistry and organic synthesis. *RSC Medicinal Chemistry*, 12(7): 1046–1064.
- Saeed, S., Rashid, N., Jones, P.G., Ali, M. & Hussain, R. (2010). Synthesis, characterization and biological evaluation of some thiourea derivatives bearing benzothiazole moiety as potential

- antimicrobial and anticancer agents. *European Journal of Medicinal Chemistry*, 45(4): 1323–1331.
- Schrödinger (2016). The PyMOL Molecular Graphics System, Version 1.8 Schrödinger, LLC.
- Smith, M. (2017). Antibiotic Resistance Mechanisms. *Journeys in Medicine and Research on Three Continents Over 50 Years*, 2017: 95–99.
- Souza, R.A.C., Costa, W.R.P., de F. Faria, E., Bessa, M. A.d.S., Menezes, R.de P., Martins, C.H.G., Maia, P.I.S., Deflon, V.M. & Oliveira, C.G. (2021). Copper(II) complexes based on thiosemicarbazone ligand: Preparation, crystal structure, Hirshfeld surface, energy framework, anti mycobacterium activity, in silico and molecular docking studies. *Journal of Inorganic Biochemistry*, 223(4): 1-13.
- Sumrra, S.H., Ibrahim, M., Ambreen, S., Imran, M., Danish, M. & Rehmani, F.S. (2014). Synthesis, spectral characterization, and biological evaluation of transition metal complexes of bidentate N, O donor schiff bases. *Bioinorganic Chemistry and Applications*, 2014: 1-11.
- Trott, O. & Olson, A.J. (2010). AutoDock Vina: improving the speed and accuracy of docking with a new scoring function, efficient optimization, and multithreading. *Journal of computational chemistry*, 31(2): 455–461. DOI: <https://doi.org/10.1002/jcc.21334>
- Wakshlak, R.B. K., Pedahzur, R. & Avnir, D. (2015). Antibacterial activity of silver-killed bacteria: the “zombies” effect. *Scientific Reports*, 5: 1–5.
- Welch, E.F., Rush, K.W., Arias, R.J. & Blackburn, N.J. (2022). Copper monooxygenase reactivity: Do consensus mechanisms accurately reflect experimental observations? *Journal of Inorganic Biochemistry*, 231(12): 1-12. DOI: <https://doi.org/10.1016/j.jinorgbio.2022.111780>
- Zeng, X. & Lin, J. (2013). Beta-lactamase induction and cell wall metabolism in Gram-negative bacteria. *Frontiers in microbiology*, 4: 128. DOI: <https://doi.org/10.3389/fmicb.2013.00128>